

# Retro-VLC: Enabling Low-power Duplex Visible Light Communication

Angli Liu  
University of Washington  
angli@cs.washington.edu

Chao Sun  
Microsoft Research, Beijing  
v-csun@microsoft.com

Jiangtao Li  
Microsoft Research, Beijing  
jiangtao.li@gmail.com

Liquan Li  
Microsoft Research, Beijing  
liqul@microsoft.com

Guobin Shen  
Microsoft Research, Beijing  
jacky.shen@microsoft.com

Feng Zhao  
Microsoft Research, Beijing  
zhao@microsoft.com

## ABSTRACT

The new generation of LED-based illuminating infrastructures has enabled a “dual-paradigm” where LEDs are used for both illumination and communication purposes. The ubiquity of lighting makes visible light communication (VLC) well suited for communication with mobile devices and sensor nodes in indoor environment. Existing research on VLC has primarily been focused on advancing the performance of one-way communication. In this paper, we present Retro-VLC, a low-power duplex VLC system that enables a mobile device to perform bi-directional communication with the illuminating LEDs over the same light carrier. The design features a retro-reflector fabric that backscatters light, an LCD shutter that modulates information bits on the backscattered light carrier, and several low-power optimization techniques. We have prototyped the [reader](#) system and made a few battery-free tag devices. [Experimental results show that the tag can achieve a 10kbps downlink speed and 0.5kbps uplink speed over a distance of 2.4m. We also outline several potential applications of the proposed Retro-VLC system.](#)

## 1. INTRODUCTION

Nowadays, white LEDs have been prevalently deployed for illumination purpose for its advantageous properties such as high energy efficiency, long lifetime, environment friendliness, to name a few. Being semiconductor devices, LEDs also possess another feature, i.e. it can be turned on and off *instantaneously* [22]. This effectively turns illuminating LED lights into a carrier and gives rise to a new “dual-paradigm” of simultaneous illumination and visible light communication (VLC). The ubiquity of illuminating infrastructure makes this dual-paradigm VLC (i.e., communication over existing lighting infrastructures) especially well suited for communication with mobile devices or sensor nodes such as streaming video to one’s mobile phone or collecting environmental data from home sensors.

Like any communication system, it is essential to have bi-directional (i.e. both LED-to-device downlink and device-to-LED uplink) communication capability to ensure reliability and flexibility. For instance, a minimum requirement

would be to acknowledge correct or incorrect reception of packets. One immediate solution would be using another medium such as a radio link to complement the VLC link. For instance, ByteLight [2], which exploits LED lighting infrastructure for both communication and localization [19, 30], has resorted to Bluetooth Low Energy (BLE) for the uplink device-to-LED communication. But such solution incurs additional cost and increased overall system complexity, and undermines the benefits of VLC such as security.

In this paper, we are interested in a bi-directional communication system solely relying on VLC. An intuitive way to realize bi-directional VLC system is to put together two one-way VLC links with reverse transmitting direction, i.e. a *symmetric solution*. It is indeed a viable solution for dedicated VLC systems. It is perhaps a widely taken assumption, as existing work on VLC has primarily been focused on improving the throughput for one-way link using power hungry, expensive, dedicated sending/receiving devices and intermediate light concentrating optical components (e.g. lenses) [7, 24, 28, 29].

However, the dual-paradigm nature of a VLC system and the practicality considerations render such symmetric solution not suitable, for two basic reasons. First, the dual-paradigm VLC system, with illumination being the primary goal, has quite asymmetric capabilities at the two ends: one end is the externally powered lighting LED and the other end is the power-constrained mobile or sensor device. Secondly, while the position of lights are usually fixed, that of a mobile or sensor node can be arbitrary and changing. In particular, the weak end cannot afford lighting up a high power LED to transmit information especially when communicating at a relative large distance (e.g. a few meters for typical indoor environments). Using optical light concentrating components may allow low-power LEDs being used, but it would require precise relative positioning and careful orienting (with the optical components being steerable) between the two ends, and is obviously impractical.

Inspired by recent work on backscatter communication systems [14, 27], in this paper, we present the design and implementation of *Retro-VLC – a low-power duplex VLC*

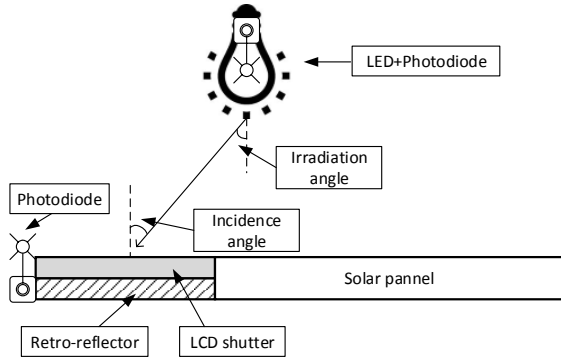


**Figure 1: System architecture.**

system that consists of a reader (ViReader) residing in the lighting infrastructure and tags (ViTags) integrated in mobile devices or sensor nodes. The ViReader is made up of an externally powered lighting LED, a light sensor (e.g. photodiode) and the control circuits. The ViTag consists of a light sensor, a retro-reflective fabric, a transparent LCD shutter and the control circuits. One example tag implementation is shown in Fig. 1.

Central to Retro-VLC is the adoption of retro-reflective fabric which retrospectively reflects light, *i.e.* bounces light back to the lighting source *exactly along its incoming direction*. Its reflecting nature helps to establish an uplink over the *same* visible light channel established by the high power lighting LED, which thus avoids using another high-power LED on the weak end and makes it possible to achieve the low-power design goal. Its retrospective nature further not only allows arbitrary relative positioning between the lighting source and the tag, but also helps to concentrate the reflected light from a scattering light source. The two favorable properties render Retro-VLC an effective visible light based backscattering communication system.

Retro-VLC works as follows. For the downlink (LED-to-tag), the LED in ViReader switches on and off at a high frequency (e.g. 1MHz, to avoid human perceptible flickering), turning the illuminating light into a communication carrier. Information bits are carried using certain modulation method (e.g. Manchester coding). The light signals are picked up by the light sensor on ViTag and decoded to restore the information. For the uplink (tag-to-LED) communication, the same carrier is leveraged via reflection. To carry bits over the reflected light carrier, we cover the retro-reflector fabric with a transparent LCD that serves as a shutter, and adopt On-Off-Keying (OOK) modulation over the reflected light carrier by controlling the passing or blocking state of the LCD shutter. The modulated reflected light carrier is then picked up by a photodiode on the ViReader and decoded by a dedicated subsystem.

Two major challenges arose in the design of the Retro-VLC system, especially the uplink. The root causes are the practicality considerations of the system and the low-power requirement of the tag. Specifically, the first challenge is

the extremely weak and noisy signal (reflected by the remote tag) received by at the ViReader. We use a photodiode with wide field of view (FoV) on the ViReader to avoid constraining the range of possible tag deployment. The wide FoV of the photodiode not only makes it less sensitive to the reflected lights (as only a tiny portion of its view actually corresponds to the retro-reflecting area of a tag), but also invites severe interference from the leakage and ambient reflection of the strong downlink signal and carrier. Secondly, the low power consumption requirement of ViTag (in hope to achieve battery-free operation by only harvesting energy from the illuminating LED) entails careful design as well. The receiving (demodulation and decoding) unit and modulation unit (the LCD) on the ViTag consume significant energy. The LCD shutter leverages the electric field to control the arrangement of liquid crystal molecules (to polarize the light). It itself is a capacitor. Frequent charging and discharging the LCD consumes relatively significant energy, especially when the refresh rate is high. In addition, for sake of cost and energy consumption, we do not use any high precision oscillator on the ViTag. There is no clock synchronization between a ViReader and ViTag (s) either.

We have addressed these challenges with the following design. We employ a differential amplifier in the ViReader receiver to filter out the noises; we adopt a multi-stage amplification design with feedbacks for automatic gain control to pull the system away from self-excitation. With these designs, we amplify the signal by up to 120dB while ensuring the stability of the system. We devise a sliding-window multi-symbol match filter to handle possible clock offsets and drifts between the ViReader and the ViTag. To achieve low power consumption of the ViTag, we have followed the principles of using as much analog components as possible, making the circuit work at the most energy-efficient (*i.e.* close to cut-off) state, and seeking maximal energy reuse. In particular, we avoid energy-demanding analog-to-digital converters (ADCs) with a specially designed comparator. The microcontroller (MCU) in ViTag handles only simple tasks such as parity check and duty cycling, and the control of LCD states. We further design an energy reuse module that collects almost half of the LCD's discharging current.

We have implemented several prototypes that demonstrate the effectiveness of our Retro-VLC design. We built battery-free ViTag device, which operates by harvesting energy from the incoming light. Fig. 1 depicts the architecture of a ViTag. It is the same size of a credit card, one-third of the area being the retro-reflector and two-thirds the polycrystalline silicon solar cell. We made two types of ViReader, modified from a normal LED bulb and a flashlight, respectively.

We evaluate our system in locations where illuminating LEDs are typically deployed such as office environments. We also evaluate in dark chambers for benchmark purpose. We measure the maximum communication range between the LED and the ViTag with various LED illumination lev-

els, ViTag orientations, solar panel areas and retro-reflector areas. Our experiments show that our  $8.2\text{cm} \times 5.2\text{cm}$  ViTag prototype can achieve  $10\text{kbps}$  downlink speed and  $0.5\text{kbps}$  uplink speed over distances of up to  $1.7\text{m}$  in dark chambers and  $2.4\text{m}$  in offices, under a  $200\mu\text{W}$  power budget. We also demonstrate its merit in security by evaluating the area around the ViTag in which uplink transmissions can be sniffed.

**Contributions:** We make the following contributions:

- We propose a practical bi-directional VLC primitive that works for small battery-free devices using retro-reflectors and LCDs and ordinary white LEDs. The design is well suited for the communication between a mobile or sensor device and the illuminating infrastructure.
- We address various challenges through energy-efficient analog circuit design and energy reuse components on the ViTag, and weak signal detection and unsynchronized decoding scheme on the ViReader.
- We build and evaluate real working prototypes, confirm the effectiveness of our design and provide a sense of its practicality.

## 2. RELATED WORK

Our work is related to prior work in VLC systems and backscatter communication systems:

**(a) VLC Systems:** Recently, there have been many efforts exploring communication mediums wherein visible lights carry information. These [work](#), however, either deal with only one-way communication without an uplink [10, 17, 20, 33], or go in a two-way fashion with both sides supplied by battery [9, 13, 21], which limit real-world practicality. Specifically, LED-to-phone systems [19, 22, 30] only support downlink transmissions, targeted at phone localization. LED-to-LED systems [31, 34] consider visible light networks, where each end is not meant to be mobile, and is not battery-free. By contrast, our work augments the existing systems with an additional uplink channel from the mobile device to the LED on the same band as the downlink, with an emphasis on the low power design and system robustness.

**(b) Backscatter Systems:** Backscattering is a way to provide transmission capability for extremely low-power devices, substituting the need for devices actively generating signals. The technique has been primarily used by RFID tags [15, 32]. Recently, Wi-Fi [16] and TV-based [23, 27] systems started employing and advancing this technique.

Our Retro-VLC system also achieves low-energy design using backscattering and further shares design principles with [16, 23, 27], that is, using analog components on the energy-constrained end. The major differences lie in the fact that we are dealing with visible light using a retro-reflector, whereas the ambient backscatter systems are backscattering radio waves. On the tag side, we use a light sensor to receive and a retro-reflector to send (by reflection) information, which is also different from the shared antenna and RF front-end in other

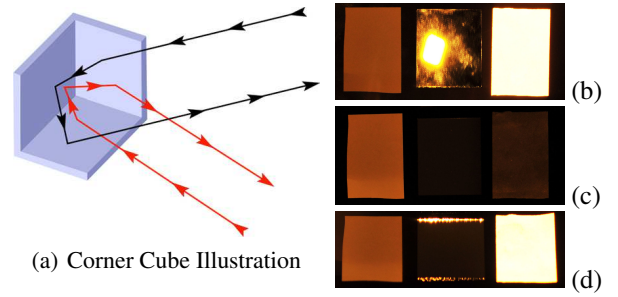


**Figure 2: Illustration of the reflection principle of a retro-reflector (a), and the comparison of the reflection property (b)-(d). The flash and camera are at positions of  $(90^\circ, 90^\circ)$ ,  $(45^\circ, 90^\circ)$  and  $(45^\circ, 45^\circ)$  in (b), (c), and (d), respectively. The three side-by-side put testing materials are, from left to right, white paper, mirror and retro-reflector fabric.**

backscattering systems. In comparison, we can easily achieve full-duplex while other systems are essentially half-duplex and require intensive tricks and significant overhead to achieve full-duplex [5, 8, 12].

In addition, because of the backscattering nature, these wireless systems tend to expose their transmissions to a wide surrounding area, leaving a good chance for side readers to overhear the information being transmitted [16, 23, 27]. By contrast, ViTag relies on visible light communication, which implies that eavesdroppers are easily discernible. The use of retro-reflectors further constraints the uplink transmission to stick along the tag-reader path. As a result, our system ViTag comes with a good security property inherently, while other systems have to enhance their security with extra efforts [25, 35].

## 3. PRELIMINARIES

Our goal is to establish a bi-directional communication link using visible lights. As the dual-paradigm nature of VLC over the lighting infrastructure entails that the primary function is illumination and the primary usage scenario is communicating with low power mobile devices or sensor nodes, we have the following two basic requirements behind the goal.

- **Efficiency Requirement:** Establish a low-power, duplex visible light communication link with a battery-free mobile end that harvests light energy from the illumination LED.
- **Practicality Requirement:** Impose no constraints on actual use. This implies a practical working range in normal indoor situations, flexible tag orientation, and that the size of the device be small.

To achieve a duplex link on visible light, one possibility is to employ a symmetric design, that is, using an LED on the mobile device or sensor node to actively emit signals,

and pick up the signals with a light sensor on the illuminating LED. Unfortunately, reaching a practical working distance (with the light typically installed on the ceiling) costs prohibitively high energy on the mobile or sensor device. The light energy attenuates quickly as the propagation proceeds [6].

One way to extend the communication range is to use directional signals, ideally a laser, or using intermediate light concentrating optical components (*e.g.* lenses). However, that would require careful alignment between the light source and the mobile device, which may further require steerable optical components and precise tag positioning. Thus, it is not quite applicable.

Another possible way towards more affordable power is to leverage the light from the illuminating infrastructure, which is usually of high power. This is similar to the design of passive RFID systems where a tag communicates with a reader by reflecting the incoming radio signal. For instance, reflecting the light using a *mirror* to a light sensor that sits beside the LED uses this principle. However, use of a mirror would then require carefully orienting the mobile device, thus violating the practicality requirement. Inspired by free space laser communication systems [3], we use a retro-reflector to meet both requirements. Below we introduce the retro-reflector and present some favorable properties about retro-reflector materials.

**Retro-reflector:** A retro-reflector is a device or surface that, unlike mirrors, reflects light back to its source along the same incoming direction with little scattering [4]. A retro-reflector can be produced using spherical lens, much like the mechanism of a cat's eye. A more feasible way to obtain retro-reflection is to use a corner reflector, which consists of a set of corner cubes each with three mutually perpendicular reflective surfaces. The principle of such a retro-reflector is shown in Fig. 2(a). A large yet relatively thin retro-reflector is possible by combining many small corner reflectors, using the standard triangular tiling. Cheap retro-reflector fabric are readily available, *e.g.* the Scotchlite series from 3M [1], and are widely used on road signs, bicycles, and clothing for traffic safety at night.

We conduct experiments to measure the reflecting properties of a retro-reflector fabric (Scotchlite 9910 from 3M). We compare it against a plain white paper which features diffusing reflection and a planar mirror that does mirror reflection. We place the three materials side by side and let the light source (a flash light) emit light at different angles while in the same distance from the materials. We capture the reflection effects with a camera from multiple angles. Fig. 2(b)-(d) shows the resulting images from experiments conducted in a dark chamber. In the figures, we can see that the retro-reflector fabric is bright as long as the light source and the camera are along the same direction, be it  $45^\circ$  or  $90^\circ$ , whereas the mirror is bright only when both the camera and the flash are at  $90^\circ$ . In the case of Fig. 2(c), the images of the mirror and the retro-reflector are dark. On the contrary, the

white paper is always slightly turned on because of its diffusion, despite the flash and camera positions. We notice that the brightness of the retro-reflector fabric tends to be weaker than that of the mirror but more uniform. This is because the fabric we used is not a perfect retro-reflector and has small dispersion [1].

The ability to bounce back light from any incidence angle leads to a favorable property of the retro-reflector: when the light source emits omni-directional lights, the retro-reflector will concentrate the lights as it reflects them. This is illustrated in Fig. 3(a). From experiments, we empirically found that the concentrated energy is directly proportional to the size of the retro-reflector fabric, as shown in Fig. 3(b).

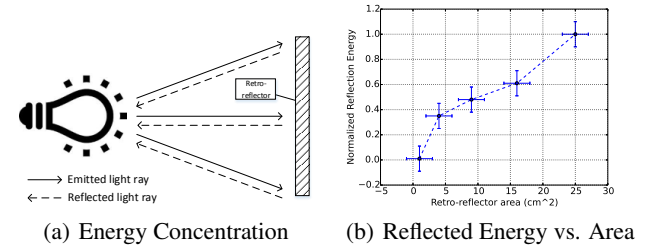


**Figure 3: Energy concentrating property of a retro-reflector when the light source emits omni-directional lights and the relationship between reflected energy and the retro-reflector size.**

**Modulating with LCD:** In terms of embedding information bits on the reflected light, special retro-reflector can alter the amplitude by electronically controlling the reflection or absorption using, for example, MEMS technologies [28, 29]. However, we hope to use ordinary, off-the-shelf retro-reflector fabrics. In order to modulate the lights reflected by such fabric, we resort to a liquid crystal display that can pass or block light under the control of the electrical field.

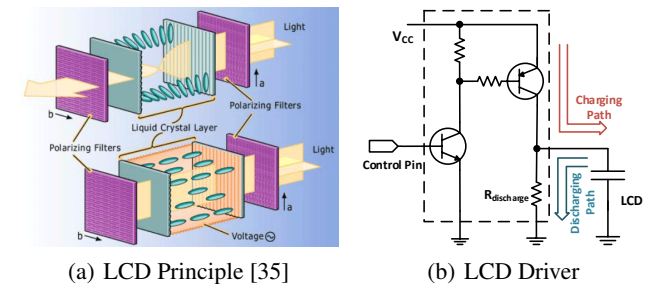


**Figure 4: The structure and principle of LCD, and its typical driving circuits.**

An LCD has a multi-layer sandwich structure. At the two ends of the LCD panel are two polarizer films; the two polarizers can be parallel or perpendicular to each other. In the middle are two glass electrodes that encompass a layer of ne-



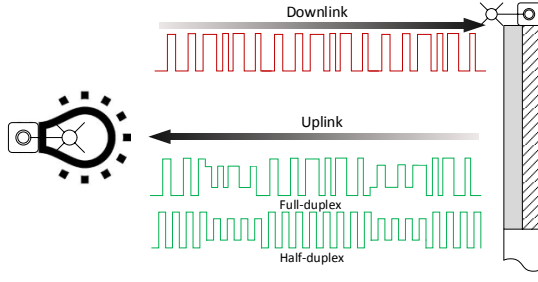


**Figure 5: Concept illustration of the Retro-VLC system.**

matic phase liquid crystals, as shown in Fig. 4(a). An LCD works as follows: when the incoming light passes through the first polarizer, it becomes polarized. Depending on the actual liquid crystal state, the polarity of the light will be changed or remain unchanged. In the natural state, liquid crystal molecules are twisted. It will change the polarity of the light passing through it. If an electric field is imposed (by the two surrounding glass electrodes) on the liquid crystal, its molecules will become untwisted. The polarity of the light will not be affected when passing through. The light will finally pass or be blocked by the second polarizer on the other end, depending on the conformance of their polarity [35].

Fig. ?? shows a typical driving circuit for charging or discharging an LCD. We use it to toggle on/off the LCD shutter. At a high level, the polarization changes with the voltage added on it: with a low voltage, the incoming light traverses the LCD and hits the retro-reflector, and the reflected light also traverses the LCD; with a high voltage, the incoming light is rejected by the LCD.

## 4. Retro-VLC OVERVIEW

The basic design of Retro-VLC is to backscatter the incoming light using a retro-reflector fabric and to modulate it with an LCD. The overall concept is illustrated Fig. 5. which depicts how our design support both half-duplex and full-duplex modes.

### 4.1 Challenges

While retro-reflecting and modulating the retro-reflected light makes it possible to establish a visible light uplink from a mobile device to the illuminating infrastructure, the actual design of Retro-VLC still faces two major challenges, rooted from the practicality and the low-power requirement of the system.

**Weak, Noisy Reflected Signal:** The signal collected by the light sensor collocating at the light source is weak (4 orders of magnitude weaker than the LED emission), due to the small size of the retro-reflector and relatively large working range. We use a photodiode with wide field of view (FoV) on the ViReader to avoid constraining the range of possible tag deployment. The wide FoV of the photodiode not only makes it less sensitive to the reflected lights (as only

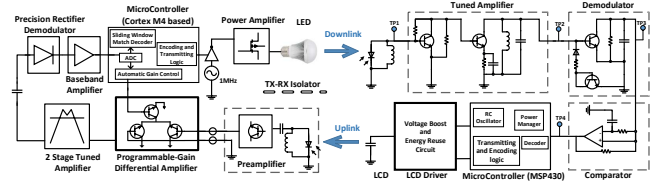


**Figure 6: Retro-VLC system architecture**

a tiny portion of its view actually corresponds to the retro-reflecting area of a tag), but also invites severe interference from the leakage and ambient reflection of the strong downlink signal and carrier. The converted electrical signal is further interfered by the harmonics of 50Hz (or 60Hz) AC current.

**Energy Efficiency:** Secondly, the low power consumption requirement of ViTag (in hope to achieve battery-free operation by only harvesting energy from the illuminating LED) entails careful design as well. The receiving (demodulation and decoding) unit and modulation unit (the LCD) on the ViTag consume significant energy. The LCD shutter leverages the electric field to control the arrangement of liquid crystal molecules (to polarize the light). It itself is a capacitor. Frequent charging and discharging the LCD consumes relatively significant energy. Its power consumption increases linearly with the refreshing rate, and consumes significant energy when operating at a high rate. In our measurement, it consumes  $84\mu A$  current at a  $500Hz$  refreshing rate.

In addition, for sake of cost and energy consumption, we do not use any high precision oscillator on the ViTag. There is no clock synchronization between a ViReader and ViTag (s) either. These consideration introduces additional challenges.

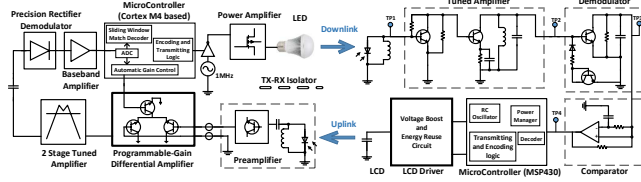
### 4.2 Principles

Inspired by design principles of some recent backscattering systems [16, 23, 27], we we apply the following design principles in addressing the challenges:

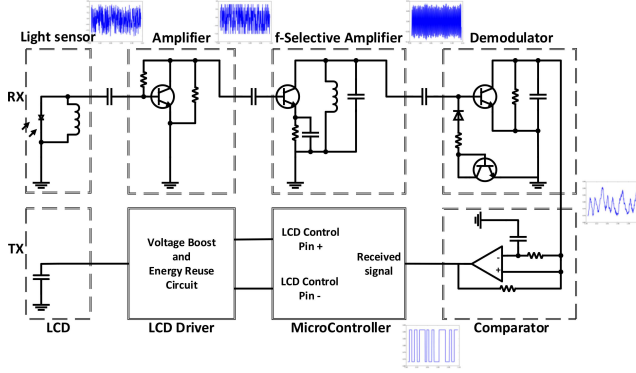
- Use analog components for signal detection. This is to avoid the expensive ADC and relieve the MCU from heavy digital signal processing.
- Make the transistors in the circuit work at a low DC operation point (*e.g.* close to cut-off state). This is an exploitation of the nonlinear relationship between the amplification gain and DC work current (hence energy consumption) of a triode.
- Reuse energy as much as possible. This is particularly to reduce LCD energy consumption.

### 4.3 Design Overview

Fig. 7 shows the architecture of a Retro-VLC system. It consists of a ViReader and a ViTag. The ViReader resides on the lighting infrastructure, consisting of an illumination LED



(a) ViReader block diagram



(b) ViTag block diagram

Figure 7: System diagram.

and transmission logic (termed ViReader-Tx hereafter), a light sensor and the subsequent receiving circuit (ViReader-Rx). The ViTag consists of a light sensor and receiving circuits (ViTag-Rx), and a retro-reflector, a modulating LCD and other circuitry components (ViTag-Tx). The ViReader-Tx and ViTag-Rx together make the *downlink* visible light channel, and the ViTag-Tx and ViReader-Rx together make the *uplink*. Retro-VLC operates as follows:

**Downlink:** For the downlink communication, the ViReader sends out information by modulating the carrier using On/Off Keying (OOK) and employing Manchester coding. This signal is captured by the light sensor of ViTag, amplified, demodulated and decoded by ViTag-Rx in analog domain.

**Uplink:** As for the uplink communication, the MCU on the ViTag controls the LCD to modulate the light carrier reflected by the retro-reflector fabric. The reflected light travels back to the light sensor that collocates with the LED. Upon capture, the weak signal is first amplified with a differential amplifier to mitigate noises, further amplified, demodulated, digitized and finally decoded. Special logic has been designed to account for the possible clock drift at the ViTag when modulating the reflected carrier as we have used a cheap RC oscillator to avoid high energy cost and overly large size of crystal oscillators.

The downlink and uplink can work concurrently on their respective bands. Hence Retro-VLC is capable of full-duplexing. Normally, when there is no traffic, the ViReader-Tx sends out the carrier by switching the LED light at a high fre-

quency  $f_0$ , which should be fast enough to avoid perceivable flickering (i.e.,  $f_0 \gg 200\text{Hz}$ ). In our implementation, we set  $f_0$  to  $1\text{MHz}$ . We support dimming of the LED by changing its DC bias. Both the receiving logic on ViReader and ViTag (when turned on) keep on monitoring their own incoming light channel. With this design, a ViTag can initiate the communication to the ViReader. An alternative design would be turning on the ViTag-Tx only when ViTag receives certain information. This is the half-duplexing mode where only the ViReader can initiate a communication session, similar to how existing RFID system works.

## 5. Retro-VLC SYSTEM DESIGN

In this section, we describe our design of Retro-VLC in more detail. The system consists of ViReader-Tx, ViReader-Rx, ViTag-Tx, and ViTag-Rx. The first two belong to the ViReader and the last two belong to the ViTag. The ViReader-Tx employs a standard design – it performs encoding using an MCU and toggles the LED light to control the power amplifier. Specifically, we employ a  $1\text{MHz}$  carrier,<sup>1</sup> use Manchester coding and perform on-off keying (OOK). The communication bandwidth we use is  $10\text{kHz}$ . We next focus on the design of the other three components, elaborating on the key design choices.

### 5.1 ViReader-Rx Design

**Challenges of ViReader-Rx Design:** The major challenges that arise in the design of the ViReader-Rx are the following. First of all, the signal from the ViTag reflection is extremely weak, especially due to the use of the small retro-reflector on the ViTag. Second, the signal is severely interfered by other light and electrical sources. In particular, as the light sensor sits next to the LED, it is likely that there is leakage from downlink signals and carrier, in addition to the diffusing reflections from the ambient sources. Because of the close distance, the interference is several orders of magnitude greater than the actual reflected signal from the ViTag. As measured, the power of the ViTag-reflected signal is about  $-80\text{dBm}$  while the ViReader-Tx emitted light signal can be up to  $30\text{dBm}$ . In fact, these interferences could cause the ViReader-Rx amplifiers to saturate without careful design. In practice, the light reflected by the movement of humans and other objects around can cause such interferences. The converted electrical signal is also interfered by commercial radios that run around  $1\text{MHz}$ . The harmonics of the  $50 - 60\text{Hz}$  AC supply of the lighting infrastructure also matters, which is on par with the toggling rate ( $0.5\text{kHz}$ ) of our LCD modulator. Thirdly, using a small and low frequency RC oscillator at the ViTag makes the reflected signal suffer from clock offsets and drifts.

In our design, we first try to isolate the receiving path, both the circuit and light sensor, from the transmitting path.

<sup>1</sup>This is a limitation from commercial off-the-shelf LED we have. If we toggle at a faster rate, the amplitude difference between On and Off state will be too small to serve as an effective carrier.

<sup>2</sup> In the rest of this section, we focus on the modular and algorithmic design of ViReader-Rx.

**Amplification and Demodulation:** As shown in Fig. 7, an external light sensor with a parallel inductor captures the ViTag signal and performs preliminary band-pass filtering. The photocurrent is then amplified by a subsequent pre-amplifier and further transmitted to the internal (*i.e.* on the ViReader board hosted within the lamp) amplifier and processing circuit. An impedance matching module is incorporated.

The pair of transmission lines is relatively long, decoupling the front end and the subsequent processing unit. As the two wires are equally affected by the common-mode noises, we thus design a tuned differential amplifier as the first-stage internal amplifier. By subtracting the signals from the two wire, the differential amplifier effectively eliminates the common-mode noises. It further suppresses other off-band noises through LC resonance at 1MHz carrier frequency. As the reflected signal from ViTag is extremely weak, we further amplify it through two additional LC-structured amplifiers. The overall amplification gain is 80dB. This signal then goes through a high precision envelope detector to pick up the baseband signal from the carrier. Finally, the baseband signal is amplified and fed to the MCU, which performs ADC processing and decodes therein.

Note that the gain of the differential amplifier is programmable and controlled by the micro-controller. We also use two-stage amplifiers (instead of one-stage amplifier with very large gain) both with feedback mechanisms. These mechanisms help pull the circuit state away from self-excitation.

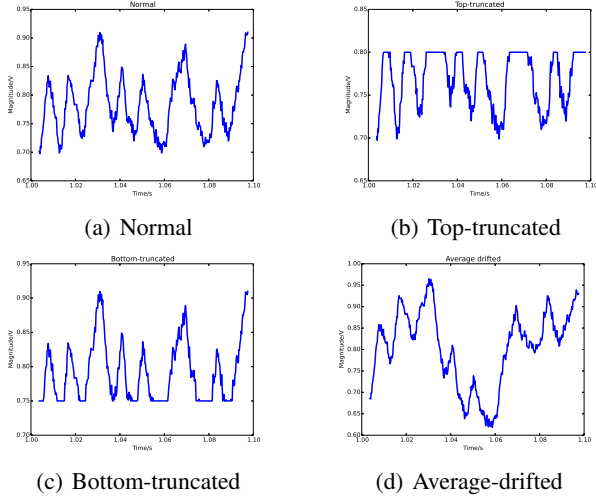


**Figure 8: Possible waveform patterns after the baseband amplifier of ViReader-Rx.**

**Decoding and Handling Clock Drift:** The clock offset and

<sup>2</sup>In practice, we use 4-layer PCB and always ensure the wires are covered by two copper layers connected to ground. We also shield the light sensor to avoid leakage of the downlink signals.

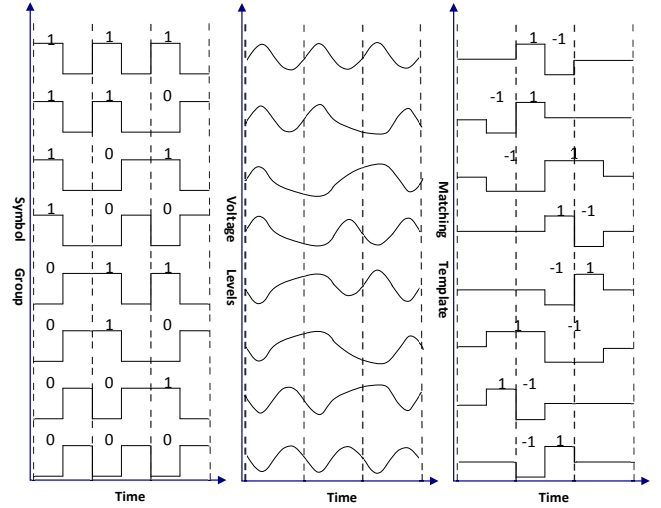


**Figure 9: All possible 3-bit patterns (left) and illustration of their actual voltage levels (middle), and corresponding matching templates (right) for edge detection.**

drift caused by the RC-clock of the ViTag bring challenges as we try to extract the timing information from the signal and perform the decoding at the same time. First, we describe why common decoding methods do not work in our case.

There are several common decoding methods. One method is perform peak (or edge) detection-based algorithm. Its principle is to extract the extreme (discontinuous) points in the signal to detect clock beats. A second approach is averaging-based algorithm in which signal samples are averaged to generate a threshold, and samples above this threshold denote ones and below denote zeros. A third approach is symbol-based match filter that tries to match the waveform of one symbol and detects the convolution peaks to determine the accurate timing.

However, none of these methods work for us. Due to the possible lag of the automatic gain control at the ViReader-Rx, the high dynamic range of interference, we may obtain top- or bottom-truncated waveforms, as shown in Fig. 8(b) and (c), or both top- and bottom-truncated waveform (not shown due to space limit). Such situation would fail peak/edge detection algorithms. Similarly, the ambient brightness changes (e.g., caused by human body reflection) will likely cause a time-varying shift in average value, this would fail the averaging-based approach. Furthermore, due to Manchester coding, one bit contains two chips – a high volt chip followed by a low volt chip, or vice versa, indicating a ‘0’ and ‘1’, respectively. Other than an all ‘0’ or all ‘1’ sequence, the rising edge and the falling edge are not evenly spaced in time. This results in two (and at most two) consecutive low (or high) voltage chips for bit sequence ‘01’ (or ‘10’). A low voltage chip corresponds to the LCD discharging phase at the ViTag; Consecutive low chips thus correspond to continuous discharging of the LCD. As a result, the second low

chip will have a lower voltage than the first one. Similarly, the second high chip will have a higher voltage than the first one in two consecutive high voltage chips. The consecutive low or high voltage chips and their corresponding voltage level are depicted in Fig. 9. In the face of these distortions, the single-symbol match filter method will fail, because the correlation peak will be skewed for those unevenly spaced high/low voltage chips.

**Sliding-window Multi-symbol Match Filter:** We develop a novel algorithm, termed sliding-window multi-symbol match filter algorithm, to decode the signal under Manchester code that's subject to a huge dynamic range. The basic idea is to avoid the biased timing caused by skewed correlation peaks in the conventional symbol-based match filter method, by matching *all possible patterns* of the waveform that may result from Manchester encoding, and iteratively adjusting the local clock by every bit period. To begin with, the algorithm exploits standard correlation to detect the preamble of a packet. Preambles last for a time period equivalent to 3 Manchester chips. Upon finding the preamble, the algorithm estimates the length of a bit using the knowledge of the ViTag clock which is known but subject to offsets and drifting. Then the algorithm iteratively performs the following two steps:

*Step 1: Template Matching.* For all the samples within the three-bit span, we match them against the corresponding template, as shown in Fig. 9. Note that the template is of amplitude of  $\pm 1$ , so as to most precisely detect the rising or falling edges of the bit in the middle. Ideally, the correlation yields a peak in the middle of the three bits.

*Step 2: Local Time Recovery.* Due to the time variance with the start of the packet and the frequency deviation between the clocks of the ViReader and the ViTag, the peak correlation does not necessarily align with the actual timing of the edge. This yields errors in clock estimation. To bound this error as the decoding goes, we perform linear regression  $t = k \cdot s + s_0$  to estimate the central time of every three bits, where  $s_0$  is the initial time estimate after preamble detection,  $s$  and  $t$  are the central time from the ViReader's view and from the ViTag's view, respectively, and  $k$  denotes the clock sampling ratio of the ViTag over ViReader. Every round  $k$  is re-estimated, and then the algorithm moves the three-bit window one bit forward.

The whole procedure is repeated till reaching the end of the packet. This time recovery algorithm bounds the error on  $t$  from diverging as the decoding process proceeds. We formally describe this in the following lemma, for which we give a proof in Appendix.

**LEMMA 5.1.** *The time recovery algorithm makes the error on the estimate for the ViTag clock converges to zero if a packet contains infinite number of bits.*

## 5.2 ViTag-Rx Design

For a normal design of ViTag-Rx, the major energy con-

sumption would be from the ADC and digital signal processing. In our design, we perform most of the processing in analog domain and avoid using the ADC while retaining accuracy. The MCU is in sleep mode for most of the time. It only wake up when a positive jump appears on the TP4 shown in Fig. 7 (i.e., output of the demodulator). Upon waking up, MCU will remember the time stamp, and together with the last wakeup time stamp it determines whether the bit received was 1 or 0, and then goes into sleep mode again, waiting to be waken up by the next incoming signal.

**Demodulation:** As shown in Fig. 7, the incoming light is first captured by the light sensor. The light sensor has an equivalent capacitance, which, with an inductor parallel to it, makes up a preliminary LC filter. Two triode amplifiers successively amplify the RF signal, after which the signal is passed along for demodulation.

Our demodulator contains a constant voltage source and a low-pass amplifier. The constant voltage source sets a ultra-low quiescent current that flows into the base of the triode in the low-pass amplifier, making it work at a critical conduction mode, so that the positive half of the signal can pass through and be amplified while the negative part can only make the triode into cut-off mode. Hence, the  $1MHz$  AC carrier is turned into the unipolar signal with a low frequency DC bias which can represent its primary envelope. Finally, the envelope signal is obtained by a smoothing capacitor and then fed into a comparator for digitization.

**Digitization and Decoding:** To avoid using power-hungry ADCs, we digitize the analog signal with a comparator. Because of the pulse-width modulation (PWM) we adopted, the goal of our design is different from a typical digitization process that involves comparison instant value against the time-average. The PWM-encoded signal uses the width of a pulse to denote bits. Specifically, a wide pulse denotes 1, and a narrow one denotes 0. To align with this pattern, we design the comparator to detect the *change* of the voltage. First, using a resistor and a capacitor, the comparator sets a time constant that features its detection delay that corresponds to the input symbol rate. The comparator consistently compares the current (analog) signal voltage  $V_{now}$  with that of the last symbol  $V_{previous}$ . If  $V_{now} > V_{previous}$ , the comparator outputs '1'; otherwise, it outputs '0'.

In summary, we achieve low energy reception at ViTag by using only analog elements and a low-power MCU (MSP430); In the analog circuit design, we further set the transistors to work at a lower DC operating point to maximally reduce energy consumption.

## 5.3 ViTag-Tx Design

Our ViTag transmitter transmits by passively backscattering the incoming light. The core of the transmitter is the combination of an LCD and a retro-reflector that serves as a modulator. While the LCD has an ultra low quiescent current, more than 70% of the power consumption during transmission is caused by LCD. The reason is that the LCD has a



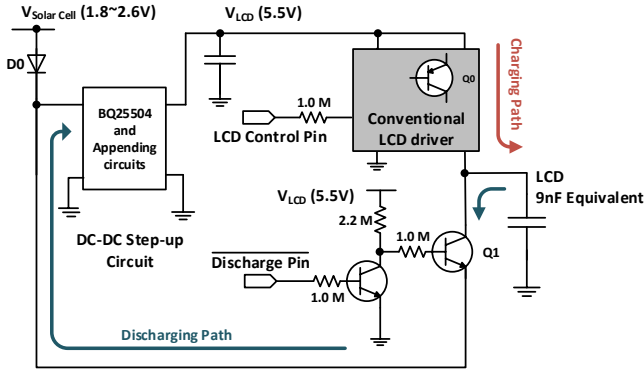


**Figure 10: Energy reuse design for LCD driver.**

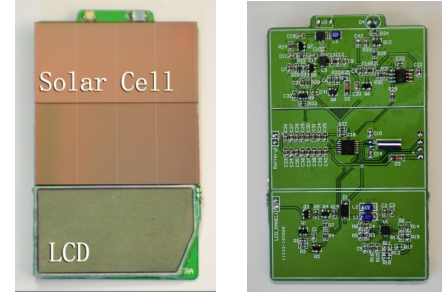
considerable equivalent capacitance ( $9nF$ ), which must be charged to  $5.5V$  to turn the LCD off and be discharged to turn the LCD on. It is this charging-discharging process that consumes energy. To conserve energy, we design an energy reuse module that recycles the discharging current. The LCD requires a voltage high enough (*e.g.* at least  $5.5V$ ) to drive it to achieve desired polarization level. This high voltage is nearly 3 times of solar cell's voltage and cannot be directly fed by solar cells. We design a voltage boosting module that achieves this. The overall design of the ViTag transmitter is presented in Fig. 7.

**Energy Reuse:** A conventional LCD driving circuit would discharge LCD from the high driving voltage to Ground and thus waste the energy. The design of our energy reuse module is depicted in Fig. 10.

During the charging phase, the DC/DC boosts voltage supplied by the solar cell to the high voltage needed for driving the LCD towards a blocking state. The MCU sets this high voltage on and activates the transistor  $Q_0$  (the PNP transistor in the conventional LCD driver module). This operation puts the LCD into the charging mode and will pump up the voltage of the LCD.

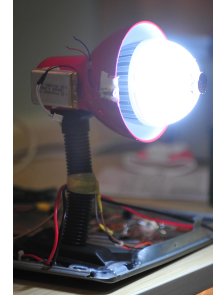
In the discharging phase, the MCU sets the  $Q_0$  to the cut-off state and thus closes the charging path, and activates the NPN transistor  $Q_1$  on the discharging path. Unlike a conventional LCD driver that discharges directly to the ground, in our design, the current flows back to the input of DC/DC circuits. This helps reduce the current drawn from the solar cell. Measurements show that the total power consumed by LCD while switching at  $0.5kHz$  decreases from  $84\mu A$  to  $46\mu A$  with energy reuse.

We note two things about our design. First, the two signals controlling the on/off state of LCD are generated by an MCU, and is alternately activated with a short interval ( $2\mu s$ ). This ensures only one transistor of  $Q_0$  and  $Q_1$  is open at a time and avoids the transient high current that would be caused if both semi-conductive transistors are activated during the switching. Second, the diode  $D_0$  is critical. It prevents the charge on the LCD from discharging to the solar



(a) ViTag Front

(b) ViTag Back



(c) Lamp



(d) Flashlight

**Figure 11: Prototype.**

cell. Without it, the initial high voltage ( $5.5V$ ) of LCD will be pull down to that of the solar cell ( $2.1V$ ) immediately after  $Q_1$  is ON, a high transient current would result and most energy would be wasted on the BE junction of  $Q_1$ .

## 6. PROTOTYPING AND POTENTIAL APPLICATIONS

### 6.1 Prototype Implementation

To demonstrate the effectiveness of our design, we implement the proposed Retro-VLC system. Our prototype is shown in Fig. 11 (a) and (b). The ViTag is battery-free and we harvest light energy using solar cell. The size of ViTag is  $8.2cm \times 5.2cm$ , same as a credit card. About two-thirds area is used for solar cells and one-third for the LCD and retro-reflector.

We use the schematics in Fig. 7 in the implementation with printed circuit boards (PCBs) and off-the-shelf circuit components, which we summarize in Table 1. The retro-reflector fabric we use is Scotchlite from 3M [1].

ViTag		ViReader	
Photodiode	BPW34	Photodiode	SFH213
MCU	MSP430G	MCU	LPC4357
DC/DC	BQ25504	MOSFET	IRF510
Comparator	TLV2762	Amplifier	LM6172, AD620
Transistor	S9018	Transistor	S9018, 2SC3357
LCD	SF110147	LED Bulb	Apollo BR30

**Table 1: Concrete models of electronic components used in Retro-VLC prototype**

Component\Voltage	2.0V	2.6V
Receiving Circuit	43.8 $\mu A$ (87.6 $\mu W$ )	48.4 $\mu A$ (125.8 $\mu W$ )
Transmitting Circuit	45.1 $\mu A$ (90.2 $\mu W$ )	36.7 $\mu A$ (95.4 $\mu W$ )
Total	91.9 $\mu A$ (183.8 $\mu W$ )	90.0 $\mu A$ (234.0 $\mu W$ )

**Table 2: Overall and component-wise energy consumption of ViTag.**

The ViReader is implemented in two forms. The first one, the lamp reader, whose transmitter is implemented with a 12W white light bulb, shown in Fig. 11 (c). The receiver is a light sensor in the centre of the lamp. It is isolated by copper foil to shelter from the light emit from the lamp directly. The second one is the flashlight reader, shown in Fig. 11 (d). It use a 3W LED as the transmitter, and its receiver contains 3 light sensors to improve the SNR to achieve longer distance. The lamp reader is designed to work with large FOV but relatively short distance (about 2.5m, 50°), while the flashlight reader is designed to work with long distance with a narrower FOV (about 10.6m, 8.5°).

The energy consumption of ViTag is related to the voltage output of solar cell. We measure the overall and component-specific energy consumption for ViTag for two typical operating voltages, as shown in Table 2. The measurement shows that the ViTag prototype indeed achieves ultra-low power consumption. With such low power consumption, we are able to drive it by harvesting light energy using small solar cells.

## 6.2 Potential Applications

The low power duplex Retro-VLC system has many potential application scenarios.

**Home sensor bearer:** Sensors such as motion, temperature, humidity *etc.* sensors can be integrated with ViTag. Sensor readings can be streamed to a ViReader-capable lighting LED. Such an application would benefit from the battery-free property of ViTag.

**Visible-light identification (VLID):** Taking visible light as the communicating media, VLID has many advantages over radio-frequency based identification systems, such as can achieve distant communication with battery free Tags, immune to electromagnetic interference, and more secure, thus it has the potential of replacing RFID in many scenarios. In warehouses, storage and transportation systems, ViTag/s as ID tags has better potential in localization accuracy and larger line-of-sight communication range than RFID.

**Interactive road side traffic signs:** The battery-free design can enable ViTag to communicate with car headlights. Similarly, it can be used for automatic tollgate.

**NFC communication/payment:** The use of visible light

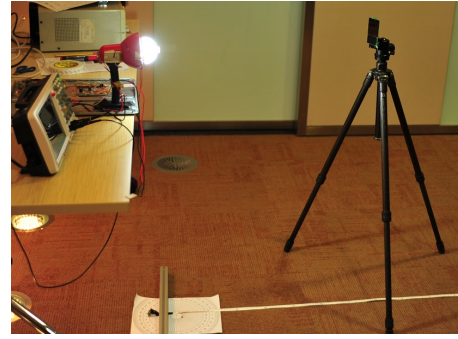


**Figure 12: Evaluation testbed setup with a pair of ViReader and ViTag.**

and the directional reflection property of the retro-reflector makes it a securer and faster means than other wireless NFC system.

## 7. EVALUATION

We evaluate Retro-VLC using our prototype implementation with a testbed shown in Fig. 12. The LED on the ViReader is 12 Watt and the ViTag is only of credit card size. As ViReader is externally powered and the downlink signal are strong, (we achieved the designed data rate 10kbps on the downlink) we have thus focused on measuring the bottleneck uplink performance. The following system aspects are evaluated, namely, packet loss rate, response time, channel response time and also the angle within which the uplink signal can be detected. The latter is to show the Retro-VLC system's ability against eavesdropping attacks. *Unless otherwise noted, evaluation about angle and response time is evaluated with the lamp reader.*

**Testing Environments:** Being a VLC system specially designed for the indoor environments with lighting structure, we carried experiments in typical office environment, where the ambient light is maintained in a comfortable range around 300lx. The ViTag harvests energy not only from the ViReader, but also from ambient light. On the other hand, the office environment comes with human movements and other disturbances that may affect communication. To give a sense of the environmental impact, we also test it in a dark chamber, as a baseline for comparison. In the dark chamber, the ViReader LED is the sole light/energy source.

**Summary of Key Findings:** The key findings are highlighted as follows:

- The experiments verify that we are able to get a ViTag to operate battery-free up to 2.4m away with lamp reader and 10.6m with flashlight reader (with package loss rate below 80%, or BER below 8.26%) and 0.5kbps data on the uplink, and the system is resilient to a wide range of ViTag orientations ( $\pm 25^\circ$ ).
- Reader-to-tag communication is resilient to eavesdropping. ViReaders can only sense the ongoing communication in a visible range, within a narrow the field of view

of about  $\pm 15^\circ$ .

## 7.1 Packet Loss Rate

In this section, we focus on evaluating the packet loss rate (PLR) of the uplink tag-to-reader communication. For VLC, the received signal strength is mainly affected by three factors, i.e., the distance between ViTag and ViReader, the incidence angle, and the irradiation angle [22].

We first measure the impact of distance on PLR by varying the distance between ViReader and ViTag. We keep the ViReader perpendicular to the ViTag, i.e.,  $0^\circ$  incidence or irradiation angles. To measure the PLR, the ViTag continuously sends packets for 20 minutes to ViReader with a constant rate. Each packet is consisted of 4bytes ID data. We count the number of packets received successfully at ViReader. Fig. 13 shows the resulting PLR versus distance.

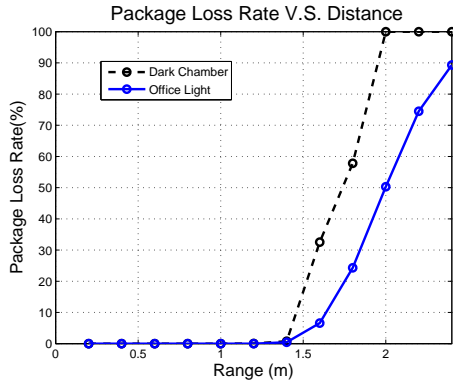


Figure 13: Distance vs. PLR of 12W LED Lamp.

Figure 13 shows that in a dark chamber, the PLR remains below 0.7% in a distance up to 1.4m. As the tag moves past 1.4m, the PLR increases dramatically; Packets are barely received beyond 1.7m. The drastic increase in PLR is because the energy obtained from the solar cell becomes insufficient in a long distance. In contrast, the PLR increases slower in the office environment thanks to the energy the ViTag harvests from the ambient light in addition to that from the ViReader.

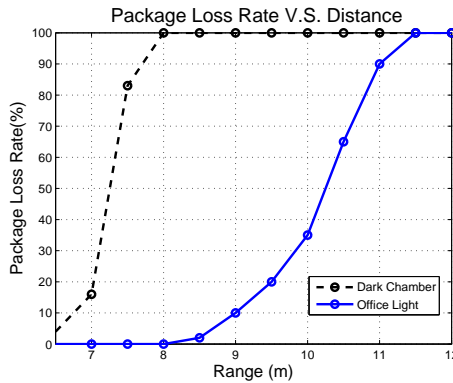


Figure 14: Distance vs. PLR of 3W flash light reader.

Figure 14 presents the PLR as a function of the range for the 3W flash-light reader. The experiment shows that with the 3W flash-light reader, a much longer communication range can be reached. Specifically, in a dark chamber, instead of 1.4m, the energy for receiving begins to drop significantly at 7.0m, and nearly exhausts at 7.4m as the PLR reaches 100%. Under the situation with normal office lights, the system performs even better in terms of the communication range. The PLR remains at nearly 0 until the tag-reader distance reaches 8.5m, and the PLR reaches 100% in a distance of 11.5m. At 10.60m, PLR reaches 80%, which is still acceptable for certain applications such as ID tag, as we can still obtain the information after a few trials.

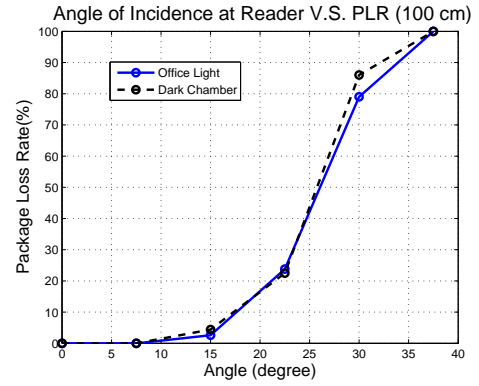


Figure 15: Angle of incidence (irradiation) vs. packet loss rate.

We then evaluate the PLR under different incidence/irradiation angles. Fix the distance between ViReader and the ViTag plane (the plane where the ViTag resides in 3D space), and move ViTag along the plane. In this setting, the incidence angle always equals the irradiation angle. In our evaluation, we fixed the distance at 100cm. The measured results are shown in Fig. 15. We note that despite the seeming high PLR (e.g. 20%), for certain applications such as ID tag, we can still obtain the information after a few trials. This is similar to RFID systems.

## 7.2 Response Time

Response time accounts for the time from the ViReader issuing a query to receiving a response from the ViTag. Therefore, the response time consists of *charging time*, downlink packet reception time, and uplink packet transmission time. Response time is a important metric for user experience. Generally, a response time below 100ms is thought to be negligible by human. In our system, due to the limitation of the LCD frequency, the uplink packet transmission time is slow, taking over 100ms to send a 32-bit ID. We envision faster LCD shutters in the future, and only focus on the charging time in the following.

If ViReader and ViTag are close enough, ViTag can quickly harvest enough energy to start conversation. Inversely, if the distance is long, ViTag needs a longer charging time before

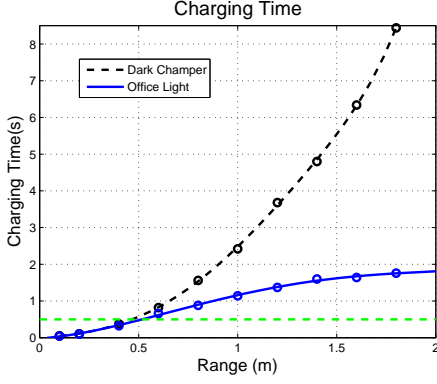


Figure 16: Charging time vs. distance in dark chamber and office room.

responding. We define the charging time as the time used to charge a **zero-initial-energy** ViTag. Charging time is affected by a number of factors like the solar cell size, ViTag energy consumption, and environment illumination level. As ViTag size is fixed, we only evaluate the impact from the environment illumination.

First we evaluate the charging time as we vary the distance from  $0.1m$  to  $1.8m$ , counting the time when the operation voltage raises from 10% to 82.5% (min operation voltage). The result is presented in Fig. 16. We can see that, when the distance is small, the charging time in both cases are close. For instance, when the distance are 10 or 20cm, the charging time are around 50 and 100ms, respectively. The two curves begin to separate after around  $0.6m$ . The charging time in office environment grows slowly due to extra energy supply from the ambient light.

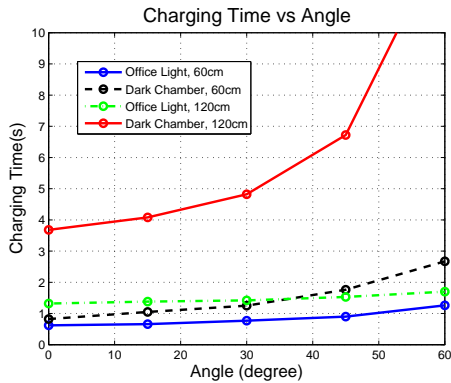


Figure 17: Charging time vs. incidence (irradiation) angles.

We note that the charging efficiency of the solar cell is also affected by the irradiation angle of the ViReader and also the incidence angle at the solar cell. For simplicity, we fix the distance between ViReader and the ViTag at 60 and 120cm, respectively, and observe charging time versus the incidence/irradiation angle shown in Fig. 17. We indeed see increase in charging time with larger angles. However,

the charging time grows slowly especially when the angle is small, e.g., below  $30^\circ$ . This means the ViTag **tolerates flexible orientations** without experiencing serious performance degradation. In particular, we see much less sensitive reaction to the angles in office environment due to energy harvest from ambient light, which further highlights the benefit of using visible light as the power source.

In practice, ViTag can always harvest energy from ambient light (sunlight or artificial lighting systems) no matter whether a ViReader exists. Thus, the actual bootstrap can be instantaneous. This is a key difference from RFID/NFC tags where the operation energy can only be gained from a dedicated reader.

### 7.3 Channel Response

For all backscatter systems, often times the energy of the signal received by the reader, which is reflected or backscattered by the tag, tends to be much weaker than the energy received by the tag, which poses a bottleneck for the system. As such, we empirically examined the received energy as a function of the communication distance. According to the light reflection model of a standalone retro-reflector shown in Fig.?? (b), the received energy attenuates proportionally to the square of the distance, which aligns with the theoretical model of the electromagnetic wave attenuation. Empirically, together with the lamp reader or the flashlight reader, however, the actual retro-reflector has a slightly diffusion angle, and the signal strength is affected by the non-linear auto-gain control (AGC) amplifier in the reader receiver.

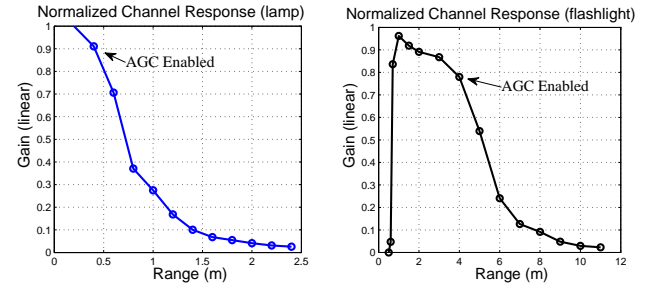


Figure 18: Normalized channel responses

To get an accurate picture of how energy diffuses as a function of the communication range, we measured the observed channel response for the lamp reader and flashlight reader. Fig. 18 shows the energy calculated by the MCU, as the square of the output voltage. It shows the nonlinearity between the square root of the reciprocal of the energy and the range, because when the signal gets too strong, the AGC suppresses the gain. Nevertheless, despite the AGC-affected part, other part of the curve attenuates close to the square of the distance.

For a typical *battery-free* backscatter system [27], the wave front of the signal transmitted by the reader is always on a circular surface, so its energy attenuates proportionally to the square of the communication range. Similarly, the modulated backscattered signal received by reader from the tag



attenuates proportionally to the square of the distance between the tag and the reader. As a result, the energy of the signal attenuates proportionally to power four of the communication range accumulatively. A detailed formula can be found in paper [26]. Therefore, for a *passive* VLC system, if we used LED as the transmitter, it would be similar to backscatter system in terms of energy attenuation; the energy received by the reader is to the power four of the communication range. However, as our experiment shows, we benefit from the fact that Retro-VLC reflects light back along the same incoming direction with little scattering, and so Retro-VLC can achieve longer communication distance than typical battery-free backscatter systems with only power two energy attenuation.

## 7.4 Maximum Working Range

We have so far evaluate both the PLR and energy harvesting. We then define the working range as the area within which the ViTag can harvest enough energy and talk with the ViReader with a chance above 20%, i.e., package loss rate is less than 80%. We measure the working range in office environment, and show the result in Fig. 19. The working range in Fig. 19 is the area within the closed blue curve. With an upright orientation of the ViTag, the maximum working distance is up to 2.6m. With ViReader perpendicular to the ViTag plane, the FoV is around 50°. In our evaluation, we always make sure the same incidence angle and irradiation angle. Thus, the measured working range is conservative. In practice, if we point the ViTag towards the ViReader, the FoV can be even larger.

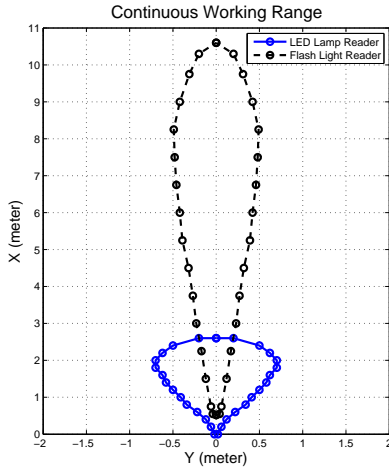


**Figure 19: Working area measured in office environment. Reader is located at (0,0).**

As to flash-light reader, the max distance from the reader to the edge of the working area is 10.6m as shown in the figure. The absolute maxim range is about 11.3m, which corresponds to 95% PLR. This can be seen in Fig. 13. Due to saturation, the flash light reader can not work if the tag-reader distance is smaller than 0.52m, as show in Fig. 19.

## 7.5 Eavesdropping Range

Eavesdropping attacks in our system refer to a device secretly listening to the conversation between ViTag and ViReader. It is shown that eavesdropping is usually an early step of other attacks like man-in-the-middle attacks [11, 18]. One of the promising applications of Retro-VLC is using ViTag as a badge or payment card. Therefore, it is important that we protect the communication safety against eavesdropping attacks.

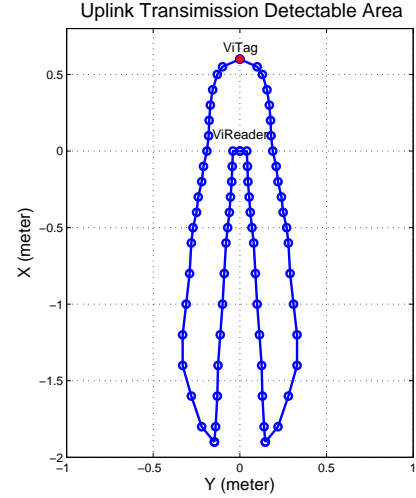


**Figure 20: Signal detection radius of uplink.**

A key feature of Retro-VLC compared with RFID/NFC is that the tag-to-reader communication is **directional**. Therefore, it is expected that a conversation from ViTag can only be detected within a narrow FoV. It is shown in [35] that a sniffer can overhear NFC communication even over 1 meter away. In our evaluation, we place a ViReader and ViTag pair 0.6m apart from each other. The ViTag faces upright to the ViReader. The setup is shown in Fig. 20. We use another reader as the attacker and measure the area where the attack can sniff the transmission from the ViTag. The area is plotted in Fig. 20.

The signal can actually be detected quite far away as shown in Fig. 20. As discussed in Fig. 13, The reason is that the retro-reflector is not perfect, it reflects the light back with a small diffusion angle. The intensity of light decays quickly with the angle. In our experiment, we use a sniffer that have 100dBm gain(the same as our ViReader ), and the result shows the detectable area is nearly 2m in the back, excluding the shadow of the ViReader . However, the whole area resides within a small FoV of the ViTag, making it much easier for the user to discern the sniffer and can be blocked by a larger cover of ViReader. Usually, the reader is fixed on the wall (e.g., a badge reader) which further reduces the signal-detectable area.

## 8. DISCUSSIONS

**Full Duplex vs Half Duplex:** Unlike radio backscattering systems where achieving full duplex is extremely challenging due to shared antenna and RF front-end, full duplexing is natural to Retro-VLC. This attributes to the fact that separate components are responsible for emitting (LED/retro-reflector) and receiving (photodiode) light. The only difference is that, in full duplexing, the reflected light contains downlink signals whereas in half duplexing, the reflected light is the pure carrier. Full duplexing also incurs extra power consumption as both the receiving and transmitting logics are active and the MCU will be kept at a high working frequency.

**Size Tradeoff:** In the ViTag implementation, we dedicate two-thirds of the area to solar cell and one-third to retro-reflector. The primary reason is that we have only access to that sized LCD (obtained from 3D glasses) and the availability of solar cells. For a target environment (mainly concerning the illumination condition) and LED power, we expect an optimal ratio between the area of the solar cell to that of retro-reflector so as to achieve maximum communication range. This is of interest when making real products.

**Working with infrared:** Since the retro-reflector, the LCD, the rx module on the tag and the rx module on the LED side can all work on the infrared band, the overall system can be used even under a totally dark condition, as long as the tx module is replaced with an infrared transmitter. This property can be beneficial in scenarios such as reading with a mobile device in the evening without bothering others' sleep, and controlling home appliances without turning on the light. In the latter scenario, ViTag works the same way as remote controls, except that ViTag can also communicate with and decode the information from ViTag-enabled devices.

## 9. CONCLUSION

In this paper, we have presented a bi-directional VLC system called Retro-VLC that consists of a modified LED (ViReader) and a tag device (ViTag). The tag can run battery-free by harvesting light energy with solar cells. The ViTag transmits by reflecting and modulating incoming light back to the LED using a retro-reflector and an LCD modulator. The system overcomes the power consumption challenge on the ViTag and interferences and clock offsets on the LED end, achieving  $10\text{kbps}$  downlink rate and  $0.5\text{kbps}$  uplink rate over a distance up to  $2.4\text{m}$ . The system also shows security advantages, preventing readers nearby from overhearing uplink data. We believe Retro-VLC have wide application scenarios.

## APPENDIX

### Appendix

**Proof of Lemma 5.1** Assume the first estimated preamble bit is at  $\hat{t}_0$ , and its actual time  $t_0$ . Denote  $s[n]$  as the central time of a three bit sequence on ViReader-Rx, and  $t[n]$  as the central time of a three bit sequence on ViTag-Tx, where  $t[n+1] - t[n]$  is the time period of one bit ( $n : 0, 1, \dots, +\infty$ ). We have

$$t[n] = t_0 + k \cdot s[n]$$

where  $k \cdot s[n]$  is a mapping from the ViReader-Rx to the actual bit boundaries, which we suppose is linear on the small bit-period time scale. The problem is then, given  $\hat{t}_0$ ,  $s$  and  $t[i]$ , estimate the next actual bit boundary  $t[i+1]$ . Our method is to approach the above equation by drawing a line that connects  $(s[i], t[i])$  and  $(0, \hat{t}_0)$  as the following

$$\hat{t}[i+1] = \hat{t}_0 + \frac{t[i] - \hat{t}_0}{s[i]} s[i+1]$$

Therefore

$$\begin{aligned} \text{error}_{\text{time}} &= \lim_{i \rightarrow \infty} \hat{t}[i+1] - t[i+1] \\ &= \lim_{i \rightarrow \infty} \hat{t}_0 + \frac{(t_0 + k \cdot s[i]) - \hat{t}_0}{s[i]} s[i+1] \\ &\quad - (t_0 + k \cdot s[i+1]) \\ &= \lim_{i \rightarrow \infty} (\hat{t}_0 - t_0) \left(1 - \frac{s[i+1]}{s[i]}\right) = 0 \end{aligned}$$

The result highlights that the deviation of the bit boundary estimate will not propagate, and will converge to zero for infinitely long packets.

## 1. REFERENCES

- [1] 3M Retro-reflector. <http://qxwujoey.tripod.com/lcd.htm>.
- [2] ByteLight. <http://www.bytelight.com/>.
- [3] Modulating Retro-reflector. [http://en.wikipedia.org/wiki/Modulating\\_retro-reflector](http://en.wikipedia.org/wiki/Modulating_retro-reflector).
- [4] Retro-reflector Principle. <http://en.wikipedia.org/wiki/Retroreflector>.
- [5] D. Bharadia and S. Katti. Full duplex mimo radios. *Self*, 1(A2):A3, 2014.
- [6] M. Born and E. Wolf. *Principles of optics: electromagnetic theory of propagation, interference and diffraction of light*. CUP Archive, 1999.
- [7] T. K. Chan and J. E. Ford. Retroreflecting optical modulator using an mems deformable micromirror array. *Journal of lightwave technology*, 2006.
- [8] J. I. Choi, M. Jain, K. Srinivasan, P. Levis, and S. Katti. Achieving single channel, full duplex wireless communication. In *MobiCom'10*.
- [9] C. Chow, C. Yeh, Y. Liu, and Y. Liu. Improved modulation speed of led visible light communication system integrated to main electricity network. *Electronics letters*, 2011.
- [10] K. Cui, G. Chen, Z. Xu, and R. D. Roberts. Line-of-sight visible light communication system design and demonstration. In *CSNDSP'10*, 2010.
- [11] A. Czeskis, K. Koscher, J. R. Smith, and T. Kohno. Rfids and secret handshakes: Defending against ghost-and-leech attacks and unauthorized reads with context-aware communications. In *CCS'08*.
- [12] M. Duarte and A. Sabharwal. Full-duplex wireless communications using off-the-shelf radios: Feasibility and first results. In *ASILOMAR'10*.

- [13] D. Giustiniano, N. O. Tippenhauer, and S. Mangold. Low-complexity visible light networking with led-to-led communication. In *Wireless Days, 2012 IFIP*, 2012.
- [14] P. Hu, P. Zhang, and D. Ganesan. Leveraging interleaved signal edges for concurrent backscatter. 2014.
- [15] S. Jeon, Y. Yu, and J. Choi. Dual-band slot-coupled dipole antenna for 900 mhz and 2.45 ghz rfid tag application. *Electronics letters*, 2006.
- [16] B. Kellogg, A. Parks, S. Gollakota, J. R. Smith, and D. Wetherall. Wi-fi backscatter: internet connectivity for rf-powered devices. In *SIGCOMM'14*.
- [17] T. Komine and M. Nakagawa. Integrated system of white led visible-light communication and power-line communication. *Consumer Electronics, IEEE Transactions on*, 2003.
- [18] K. Koscher, A. Juels, V. Brajkovic, and T. Kohno. Epc rfid tag security weaknesses and defenses: passport cards, enhanced drivers licenses, and beyond. In *CCS'09*.
- [19] Y.-S. Kuo, P. Pannuto, K.-J. Hsiao, and P. Dutta. Luxapose: Indoor positioning with mobile phones and visible light. *MobiCom'14*.
- [20] H. Le Minh, D. O'Brien, G. Faulkner, L. Zeng, K. Lee, D. Jung, Y. Oh, and E. T. Won. 100-mb/s nrz visible light communications using a postequalized white led. *Photonics Technology Letters, IEEE*, 2009.
- [21] H. Li, Y. Liu, T. Xing, Y. Wang, J. Uribe, H. Baghaei, S. Xie, S. Kim, R. Ramirez, and W.-H. Wong. An instantaneous photomultiplier gain calibration method for pet or gamma camera detectors using an led network. In *Nuclear Science Symposium Conference Record. IEEE*, 2003.
- [22] L. Li, P. Hu, C. Peng, G. Shen, and F. Zhao. Epsilon: a visible light based positioning system. In *NSDI'14*.
- [23] V. Liu, A. Parks, V. Talla, S. Gollakota, D. Wetherall, and J. R. Smith. Ambient backscatter: wireless communication out of thin air. In *SIGCOMM'13*.
- [24] D. N. Mansell, P. S. Durkin, G. N. Whitfield, and D. W. Morley. Modulated-retroreflector based optical identification system, 2002. US Patent 6,493,123.
- [25] R. Nandakumar, K. K. Chintalapudi, V. Padmanabhan, and R. Venkatesan. Dhvani: secure peer-to-peer acoustic nfc. In *SIGCOMM'13*.
- [26] P. V. Nikitin and K. S. Rao. Theory and measurement of backscattering from rfid tags. *Antennas and Propagation Magazine, IEEE*, 48(6):212–218, 2006.
- [27] A. N. Parks, A. Liu, S. Gollakota, and J. R. Smith. Turbocharging ambient backscatter communication. In *SIGCOMM'14*.
- [28] W. S. Rabinovich, G. C. Gilbreath, P. G. Goetz, R. Mahon, D. S. Katzer, K. Ikossi-Anastasiou, S. C. Binari, T. J. Meehan, M. Ferraro, I. Sokolsky, et al. Ingaas multiple quantum well modulating retro-reflector for free-space optical communications. In *International Symposium on Optical Science and Technology*. International Society for Optics and Photonics, 2002.
- [29] W. S. Rabinovich, R. Mahon, P. Goetz, E. Waluschka, D. Katzer, S. Binari, and G. Gilbreath. A cat's eye multiple quantum well modulating retro-reflector. Technical report, DTIC Document, 2006.
- [30] N. Rajagopal, P. Lazik, and A. Rowe. Visual light landmarks for mobile devices. In *IPSN'14*.
- [31] S. Schmid, G. Corbellini, S. Mangold, and T. R. Gross. Led-to-led visible light communication networks. In *MobiHoc'13*.
- [32] L. Ukkonen, M. Schaffrath, D. W. Engels, L. Sydanheimo, and M. Kivikoski. Operability of folded microstrip patch-type tag antenna in the uhf rfid bands within 865-928 mhz. *Antennas and Wireless Propagation Letters, IEEE*, 2006.
- [33] J. Vučić, C. Kottke, S. Nerreter, K.-D. Langer, and J. W. Walewski. 513 mbit/s visible light communications link based on dmt-modulation of a white led. *Journal of Lightwave Technology*, 2010.
- [34] Q. Wang, D. Giustiniano, and D. Puccinelli. Openvlc: software-defined visible light embedded networks. In *VLCS'14*.
- [35] R. Zhou and G. Xing. nshield: a noninvasive nfc security system for mobile devices. In *MobiSys'14*.